Construction and Building Materials 125 (2016) 613–624

Contents lists available at ScienceDirect

Construction and Building Materials

journal homepage: www.elsevier.com/locate/conbuildmat

Modelling of change in permeability induced by dilatancy for brittle geomaterials

S. Rahal [a,b,*], A. Sellier [b], J. Verdier [b]

[a] Institut de Recherche en Génie Civil et Mécanique (GeM), Université de Nantes, École Centrale de Nantes, CNRS: UMR 6183, 58 rue Michel Ange, 44600 Saint-Nazaire, France
[b] Université de Toulouse, UPS, INSA, LMDC (Laboratoire Matériaux et Durabilité des Constructions), 135, avenue de Rangueil, F-31 077 Toulouse Cedex 04, France

HIGHLIGHTS

- The computed permeability increases in function of plastic dilatancy.
- The induced anisotropic permeability tensor is computed according to the directions of non-isotropic expansions.
- The crack spacing in geomaterials decreases when the size of "inclusions" decreases.

ARTICLE INFO

Article history:
Received 18 May 2016
Received in revised form 29 July 2016
Accepted 1 August 2016
Available online 26 August 2016

Keywords:
Permeability
Cracking
Dilatancy
Anisotropy
FEM

ABSTRACT

The safety and durability of concrete structures are significantly affected by cracking. This structural disorder provides a preferential path for the penetration of fluids and may accelerate the material deterioration. This study investigates the mechanical damage and permeability interactions in geomaterials subjected to compressive stress inducing cracking. The development reported here is implemented within an elasto-plastic damage model able to compute plastic dilatancy. The model assumes an initial isotropic permeability tensor which becomes anisotropic with non-isotropic expansion. The model capabilities are highlighted by simulating uniaxial and triaxial compression tests. The simulation results are compared with experimental data.

1. Introduction

Cracking in civil engineering structures significantly affects their durability and ultimately their safety. When cracks reach the reinforcement, the load-bearing capacity is decreased and the material deterioration can accelerate. Regarding the transfer properties, cracking leads to leaks and loss of containment ability induced by the increasing permeability as cracks open.

Several experimental studies have been carried out in order to predict the change of permeability caused by damage. For instance, in the case of a localized crack initiated by a split test, it has been shown that permeability variations can be expressed as a function of crack opening [1–6]. When a laminar flow of water or gas is considered, Poiseuille's law has been found appropriate to predict flow rate through the macroscopic crack [3–6].

On the other hand, diffuse cracking, which is the focus of this paper, is usually generated by uniaxial or deviatoric loading [7–15]. In this situation, it has been shown that the change of permeability can be expressed as a function of a damage parameter, D, proportional to the variation of Young's modulus [10,12,16]. This parameter quantifies the loss of stiffness induced by cracking. It is a scalar quantity, the value of which can range between 0 (healthy material) and 1 (completely damaged material). For instance, exponential [10,12] and logarithmic [16] empirical functions have been proposed to manage permeability variations with respect to the variable, D.

The experimental results found in [10,12,13] are plotted in Fig. 1 and compared to the proposed empirical functions with respect to D. These relationships were assumed to be appropriate only when $D \in [0 - 0.15]$. As shown in Fig. 1, the ratio of permeabilities between the damaged and healthy samples $\left(k/k^0\right)$ remains lower than 9 in the pre-peak phase, and does not change significantly with the type of concrete: plain concrete (OC), high-performance concrete (HPC) or high-performance fibre-reinforced concrete (HPFRC) [10]. Other authors [12,13] have found that the

---

* Corresponding author at: Institut de Recherche en Génie Civil et Mécanique (GeM), Université de Nantes, École Centrale de Nantes, CNRS: UMR 6183, 58 rue Michel Ange, 44600 Saint-Nazaire, France.
E-mail address: rahal-s@univ-nantes.fr (S. Rahal).
URL: https://gem.ec-nantes.fr/ (S. Rahal).

http://dx.doi.org/10.1016/j.conbuildmat.2016.08.002
0950-0618/

Nomenclature

Name	Symbol
$\mathbb{C}$	fourth-order stiffness tensor
$\boldsymbol{\varepsilon}^e$	elastic strain tensor
$\boldsymbol{\varepsilon}^{pl,s}$	plastic strain tensor including dilatancy
$\boldsymbol{\sigma}$	total stress tensor
$\tilde{\boldsymbol{\sigma}}$	undamaged stress tensor
$\tilde{\boldsymbol{\sigma}}^d$	deviatoric part of the undamaged stress tensor $\tilde{\boldsymbol{\sigma}}$
$\mathbf{k}^{\text{eq,s}}$	induced anisotropic permeability tensor due to dilatancy
f^{DP}	Drucker–Prager plastic criterion
δ	Drucker–Prager coefficient
ϕ	friction angle
F^{DP}	non-associated Drucker–Prager yield function
β	dilatancy coefficient
d^s	isotropic shear damage
$\varepsilon^{th,s}$	dilatancy threshold used to compute d^s
$\varepsilon^{k,s}$	characteristic strain used to compute d^s
$\varepsilon^{th,p}$	strain percolation threshold used to compute $\mathbf{k}^{\text{eq,s}}$
Δ_{jj}	equivalent crack spacing in the j direction
Δ	isotropic equivalent crack spacing used to compute $\mathbf{k}^{\text{eq,s}}$
k^0	initial isotropic permeability
k_i^{F}	permeability of the ith crack
w_{jj}^i	crack opening of the ith crack in the j direction
Q_j^{tot}	total flow in the j direction
Q_j^0	flow through the healthy part of the material in the j direction
Q_j^{F}	flow through the cracks in the j direction
ℓ_{jj}	size of the finite element in the j direction
n	number of cracks
E^0	initial isotropic Young's modulus
ν^0	initial isotropic Poisson's ratio
R_0^c	threshold stress to initiate plastic dilatancy
R^c	compression peak strength
$\varepsilon^{\text{peak,c}}$	strain at R^c
σ^0	confining pressure

ratio $\left(k/k^0\right)$ remains lower than 4 (for plain concrete). As will be shown in the next section, these differences can be attributed to the directions of flow measurements (according to the induced anisotropy of cracking in a uniaxial compression test). For instance, in reference [10], the measurements were carried out in the same direction as loading, while in references [12,13], the authors made them in the direction perpendicular to the loading.

When $D \in [0.15 - 1]$, especially after the peak of the behaviour law, the literature provides a group of empirical relationships which have to be fitted according to experimental results and finite element sizes in order to predict realistic permeability variations [17,20,19]. As shown in Fig. 2, the empirical logarithmic function proposed in [19] gave a reasonable fit for the experimental permeability variations under the uniaxial compression test found in [12]. The relationship proposed in [16], which was fitted on tensile test [18,21] (see [21] for more details on the experimental device) also seemed to give good agreement with measurements too. We recall that, in pre-peak phase, this relation was fitted on a uniaxial compression test [10].

In a first step, the mechanisms observed to be involved during uniaxial compression or deviatoric loading leading to increased permeability are highlighted and the drawbacks of previous simplified damage formulations are pointed out. The second step of this work focuses on the proposed anisotropic permeability model, which is fundamentally based on the damage model [22] enhanced by a coupling with non-standard plasticity (implemented in CAST3M finite element program [23]). The model results are compared to mechanical and permeability measurements. Finally, triaxial tests are simulated in order to demonstrate the relevance of such modelling.

2. Change of permeability under compression loading

2.1. Drawback of damage-permeability relationship

As suggested by experimental results [10,12,14] and usually adopted in numerical modelling, the change of permeability can

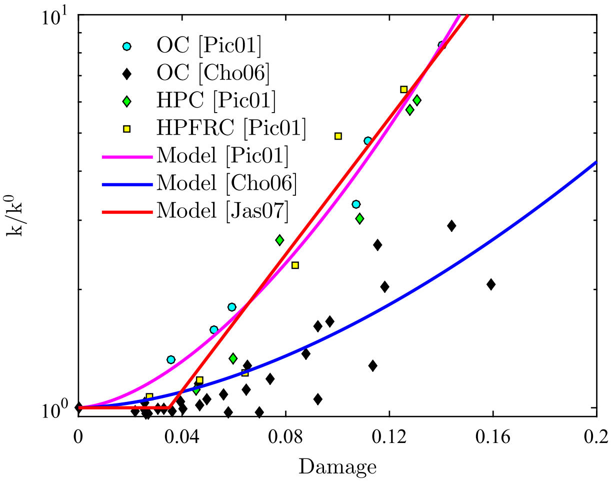

Fig. 1. Predicted variations of permeability ratio $\left(k/k^0\right)$ [10,12,16] with respect to the damage parameter: comparison with experimental permeability measurements [10,12].

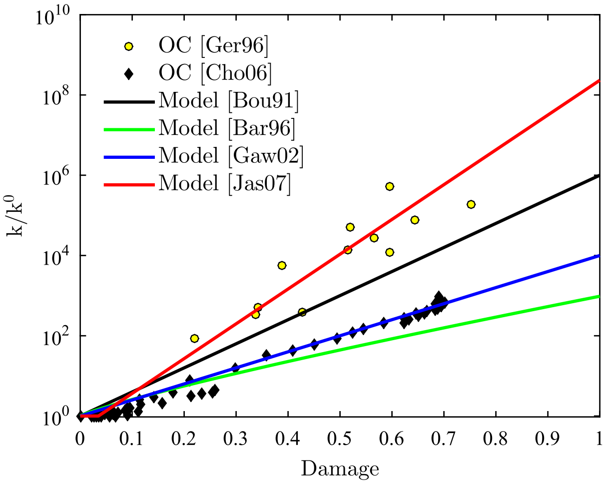

Fig. 2. Predicted variations of permeability ratio $\left(k/k^0\right)$ [17–19,16] with respect to the damage parameter: comparison with experimental permeability measurements [18,12].